VOL. 12, NO. 18, SEPTEMBER 2017 ISSN 1819-6608
ARPN Journal of Engineering and Applied Sciences


www.arpnjournals.com

THE EFFECT OF INLET ASPECT RATIO (R_{IA}) TO THE THREE DIMENSIONAL MIXING CHARACTERISTICS IN TANGENTIAL BURNER

Pasymi[1,2], Yogi Wibisono Budhi[1] and Yazid Bindar[1]
[1]Department of Chemical Engineering, Faculty of Industrial Technology, Institut Teknologi Bandung, Bandung, Indonesia
[2]Department of Chemical Engineering, Faculty of Industrial Technology, Bung Hatta University, Padang, Indonesia
E-Mail: yazid@che.itb.ac.id

ABSTRACT

The degree of mixing is one of the main indicators of the combustion performance in a combustion chamber. The higher the degree of mixing, the more intensive the contact/reaction between the air and the fuel, so that the combustion performance is getting better. The degree of mixing in a combustion chamber is indicated quantitatively by several variables such as the velocity profiles, the flow structure and the turbulence intensity. The degree of mixing in a combustion chamber is influenced by the factors of geometries and operating conditions. This study is aimed to determine the effect of the inlet aspect ratio (R_{IA}) to the mixing characteristics in a tangential burner. The investigation methodology used in this study is based on the numerical simulation with the Ansys-Fluent simulation code as a Computational Fluid Dynamics (CFD) engine. The fluid flow modelings are performed with the standard k-ε turbulent model. From the simulations that at mesh interval size smaller than 7 % of the chamber diameter, the standard k-ε model is able to match satisfactorily the tendency of the experimental velocity profiles available in the literature. The simulation results also show that the inlet aspect ratio has a significant influence to the mixing characteristics in the tangential burner. Within the R_{IA} value that is tested, the best mixing characteristic is found on the burner with the R_{IA} value of 10. The formation of the tornado tail flow structure is determined by the inlet aspect ratio, the total mass flow rate and the swirl number.

Keywords: computational fluid dynamic, inlet aspect ratio, recirculation flow structure, turbulence intensity, mixing characteristic.

INTRODUCTION

The biomass steam power plant is the most reliable power plant to meet the needs of the electricity for small islands and remote areas in the future. Beside, the environmentally friendly (CO_2 neutral) reason and relatively cheap production cost, the biomass-based power plant has a high empowerment degree. The empowerment degree of the biomass steam power plant is much higher than the other small-scale power plants, such as an hydro-based power plant, a wind-based power plant, and a solar-based power plant. According to Tokarski *et al*. (2015), the biomass steam power plant can be operated with a constant load for ± 7,000 hours per year, the wind-based power plant is able to be operated for 2,500 hours per year and the solar-based power plant is only available for 700 hours per year [1].

The core of the biomass steam power plant technology lies on the design of the boiler furnace. From three kinds of the boiler furnace design, namely grate boiler furnace, fluidized boiler furnace and suspended boiler furnace, the appropriate boiler furnace design for the biomass steam power plant is suspended boiler furnace [2]. In this type of the boiler furnace, the fuel supply to the furnace is delivered through a burner. As well as fuel supply, a burner also serves as the ignition trigger.

One of the factors that influences the combustion performance inside the burner is the fluid dynamic characteristics. These characteristics affect the process of the fuel transportation, the fuel mixing, and the fuel combustion [3]. In order to increase the burner performance, tangential flows are often involved in the burner. It functions to increase the degree of mixing and has a positive impact on the combustion performance.

The tangential flow characteristics in a burner are determined by the geometries and the operating conditions. The geometry factors that affect the tangential flow characteristics in a burner are the cylinder ratio, the inlet geometry especially the geometry of tangential inlet, and the outlet geometry. While the operating conditions which affect the flow characteristics are the total mass flow rate and the swirl number (Sn) or sometimes introduced as the initial tangential intensity (I_{TI}).

Although there has been a lot of researches related to the tangential flow characteristics, but the influence of the inlet aspect ratio (R_{IA}) to the fluid flow characteristics in the combustion chamber has not been studied experimentally or numerically. This study is aimed to quantify the effect of inlet aspect ratio on the mixing characteristics in a tangential burner. The variables that quantify the mixing characteristics are the velocity profile, the flow structure, the turbulence intensity and the other relevant variables.

LITERATURES REVIEW

Fluid dynamic characteristics

Fluid dynamic characteristic is an important factor in the design and the operation of a burner. This fluid characteristic largely determines the sustainability of the processes that occur in the burner, including the mixing process. The degree of mixing in a burner is influenced by the geometry and the operating condition.

Some of the indicators which are often used to express the fluid mixing characteristics, among others, are

the velocity profiles, the velocity vectors, the flow pathlines, the turbulence intensity, and the spurt pattern. The higher the degree of mixing, the higher the combustion performance inside the burner is.

The tornado tail flow structure as a type of the recirculation flow is one of the important flow characteristic which determine the degree of mixing. The existence of such this recirculation flow pattern is visualized by plots of the velocities, the plot of the turbulence intensity, the isosurface of the velocity vectors and the three dimensional flow pathlines.

The axial velocity profiles indicate the presence of the recirculation flow. If the axial velocity has a negative sign, this means that the recirculation flow occurs. So that the axial velocity profile can be used to describe the recirculation flow pattern.

The turbulence intensity is considered to quantify the degree of the flow mixing. The higher the value of the turbulence intensity, the higher the degree of the flow mixing and vice versa. The turbulence intensity (I) is defined as the ratio between the root-mean square of the the summation of the squares of x, y and z velocity fluctuations to the mean flow velocity magnitude [4]. A turbulence intensity of 1% or less is generally considered as a low turbulence intensity. A turbulence intensity greater than 10% is classified as a high turbulence intensity.

The spurts pattern at the burner outlet is an important variable to the overall combustion performance of the boiler furnace. This pattern is responsible for the completion of the combustion process in the boiler furnace. To complete the combustion process in the boiler furnace, the flow pattern at the burner outlet should be spread out well.

This field of the study attracts the attention of many researchers such as Chen *et al*. [5], Nemoda *et al.* [6], Escudier *et al.* [7], Vazquez [8] and Bourgouin *et al.* [9]. Chen [5] investigated experimentally and numerically the effects of the initial tangential intensity on the flow pattern in the combustion chamber. The flow pattern was reported to be very sensitive to the I_{TI} value and to the number of the tangential inlet. The higher the swirl number and the higher the amount of tangential inlet, the easier the formation of a symmetric flow is [5].

Another study on the effect of swirl number to the flow structure in a combustion chamber was conducted by Nemoda *et al*. (2005). They stated that the recirculation flow in the combustion chamber was formed only at a high swirl number ($S \geq 2.48$). This flow structure is indicated to have a positive impact on the chemical conversion and on the flame stability in the combustion process [6].

Escudier [7] investigated the effect of the outlet contraction on the flow profiles in the swirl chamber. For high swirl flows, the outlet contraction affects the flow profiles significantly. The effect of the operating conditions on the flow structure in the combustion chamber was studied by Vazquez [8] using a simulation method. The flow structure inside the combustion chamber is formed by a vortex pattern in the centre of the chamber and a spiral pattern near the wall [8].

Bourgouin *et al.* [9] conducted the experimental and simulation work on the effect of the swirler geometry on the flow structure in the combustion chamber. The velocity profiles and the frequency of the precessing vortex core (PVC) were found to be very sensitive to the swirler geometries. The longer the swirler blade, the higher the angular and the axial velocities are. This leads to the higher the frequency of PVC [9].

Fluid dynamic modeling

The CFD method is very powerful as an investigation computational engine to generate three dimensional fluid dynamics characteristics. This method is able to provide comprehensive data in a relatively low cost and shorter time effort. The advances in the computer technology and the reliability of the existing computational techniques allow the CFD method to be performed using an ordinary computer (PC or laptop) with the acceptable results.

The performances of a turbulence model are affected by several factors such as a geometry shape, an operating condition and a numerical parameter. There is no single turbulence model that can work well for all geometries and operating conditions. Therefore, the turbulent model for a certain case must be evaluated first properly.

Nemoda declared that for an atmospheric swirl burner, the predictions of *k-ε* models (standard and RNG) for the axial and the tangential velocities are better than the RSM model [6]. While, Reis *et al*. [10] stated that the standard k-ε turbulence model satisfactorily represents the experimental data of an industrial burner. The computational effort that is required for the standard k-ε turbulence model is less than that of RNG k-ε turbulence model [10]. Based on the issues that is described above, the standard k-ε turbulence model is proven to be more practical, robust and reliable by comparing to the others.

There will be six conservation equations to be solved if the fluid dynamic characteristics are modeled using the standard k-ε turbulence model. There are namely one equation for the mass conservation, Equation. (1), three equations for the momentum conservation, Equation. (2) to Equation. (4), one equation for the conservation of the specific turbulent kinetic energy, Equation. (5) and one equation for the conservation of the turbulent kinetic energy dissipation rate, Equation. (6). To close these six conservation equations, two constitutive model equations, Equation. (7) and Equation. (8) are needed. The mentioned equations above are written as follows:

$$\frac{\partial \bar{u}_x}{\partial x} + \frac{\partial \bar{u}_y}{\partial y} + \frac{\partial \bar{u}_z}{\partial z} = 0 \quad (1)$$

$$\rho \frac{\partial \bar{u}_x}{\partial t} + \rho \bar{u}_x \frac{\partial \bar{u}_x}{\partial x} + \rho \bar{u}_y \frac{\partial \bar{u}_x}{\partial y} + \rho \bar{u}_z \frac{\partial \bar{u}_x}{\partial z} = -\frac{\partial \bar{p}}{\partial x} + \frac{\partial}{\partial x}\left[\mu_{eff} \frac{\partial \bar{u}_x}{\partial x}\right] +$$

$$\frac{\partial}{\partial y}\left[\mu_{eff}\frac{\partial \bar{u}_x}{\partial y}\right] + \frac{\partial}{\partial z}\left[\mu_{eff}\frac{\partial \bar{u}_x}{\partial z}\right] + \rho g_x \quad (2)$$

$$\rho\frac{\partial \bar{u}_y}{\partial t} + \rho\bar{u}_x\frac{\partial \bar{u}_y}{\partial x} + \rho\bar{u}_y\frac{\partial \bar{u}_y}{\partial y} + \rho\bar{u}_z\frac{\partial \bar{u}_y}{\partial z} = -\frac{\partial \bar{p}}{\partial y} + \frac{\partial}{\partial x}\left[\mu_{eff}\frac{\partial \bar{u}_y}{\partial x}\right] + \frac{\partial}{\partial y}\left[\mu_{eff}\frac{\partial \bar{u}_y}{\partial y}\right] + \frac{\partial}{\partial z}\left[\mu_{eff}\frac{\partial \bar{u}_y}{\partial z}\right] + \rho g_z \quad (3)$$

$$\rho\frac{\partial \bar{u}_z}{\partial t} + \rho\bar{u}_x\frac{\partial \bar{u}_z}{\partial x} + \rho\bar{u}_y\frac{\partial \bar{u}_z}{\partial y} + \rho\bar{u}_z\frac{\partial \bar{u}_z}{\partial z} = -\frac{\partial \bar{p}}{\partial z} + \frac{\partial}{\partial x}\left[\mu_{eff}\frac{\partial \bar{u}_z}{\partial x}\right] + \frac{\partial}{\partial y}\left[\mu_{eff}\frac{\partial \bar{u}_z}{\partial y}\right] + \frac{\partial}{\partial z}\left[\mu_{eff}\frac{\partial \bar{u}_z}{\partial z}\right] + \rho g_z \quad (4)$$

$$\frac{\partial k}{\partial t} + \rho\bar{u}_x\frac{\partial k}{\partial x} + \rho\bar{u}_y\frac{\partial k}{\partial y} + \rho\bar{u}_z\frac{\partial k}{\partial z} = \frac{\partial}{\partial x}\left[\frac{\mu_{eff}}{\sigma_k}\frac{\partial k}{\partial x}\right] + \frac{\partial}{\partial y}\left[\frac{\mu_{eff}}{\sigma_k}\frac{\partial k}{\partial y}\right] + \frac{\partial}{\partial z}\left[\frac{\mu_{eff}}{\sigma_k}\frac{\partial k}{\partial z}\right] + P_k - \rho\varepsilon \quad (5)$$

$$\rho\frac{\partial \varepsilon}{\partial t} + \rho\bar{u}_x\frac{\partial \varepsilon}{\partial x} + \rho\bar{u}_y\frac{\partial \varepsilon}{\partial y} + \rho\bar{u}_z\frac{\partial \varepsilon}{\partial z} = \frac{\partial}{\partial x}\left[\frac{\mu_{eff}}{\sigma_\varepsilon}\frac{\partial \varepsilon}{\partial x}\right] + \frac{\partial}{\partial y}\left[\frac{\mu_{eff}}{\sigma_\varepsilon}\frac{\partial \varepsilon}{\partial y}\right] + \frac{\partial}{\partial z}\left[\frac{\mu_{eff}}{\sigma_\varepsilon}\frac{\partial \varepsilon}{\partial z}\right] + C_{\varepsilon 1}\frac{\varepsilon}{k}P_k - C_{\varepsilon 2}\rho\frac{\varepsilon^2}{k} \quad (6)$$

$$\mu_t = C_\mu\rho\frac{k^2}{\varepsilon} \quad (7)$$

$$\mu_{eff} = \mu + \mu_t$$

The $\bar{u}_x$, $\bar{u}_y$ and $\bar{u}_z$ are the mean velocity components in x, y and z directions. $\bar{p}$ is the mean pressure. k is the specific turbulent kinetic energy. ε is the dissipation rate of the turbulent kinetic energy. The variables μ and ρ are the fluid viscosity and the fluid density, respectively. While μ_t is the turbulence viscosity. C_μ is an empirical constant.

In the numerical simulation, the simulated results may be sensitive to several numerical parameters, such as the pressure-velocity coupling scheme, the spatial discretization scheme, the mesh type, the mesh interval size, and the wall function [4]. The mesh interval size is the most sensitive numerical parameter to the simulation results. Too large the mesh interval size leads to less accurate predictions. Contrary, too small the mesh interval size will give very accurate predictions but it requires a huge computational effort. Therefore, the mesh interval size optimization needs to be done.

MATERIALS AND METHODS

Materials

The materials and equipment required for the implementation of these fluid flow simulation are the CFD software and the hardware. The CFD software is the Anyst Fluent CFD. The geometry and mesh generation is conducted using the Gambit mesh generation software to transform the physical geometry of the designed burner into the geometry and meshed form to be inputed to the Ansys Fluent CFD engine.

The computer hardware is only an ordinary laptop computer. This computer has a quad Core-i7 2.2 Ghz processor, a Nvidia-GTX graphic processor and 8 GB Ram.

Methods

The numerical simulation is begun by evaluating the effect of numerical parameters on the performance of the standard k-ε turbulence model. This needs to be done in order to get the best model performance. Some numerical parameters evaluated here are pressure-velocity coupling scheme, spatial discretization scheme, mesh type, and mesh interval size.

The next step of the simulation is to quantify the effect of inlet aspect ratio to the mixing characteristics in the tangential burner. The designed geometry of the tangential burner for this study is shown in Figure-1.

The diameter of the burner cylinder is 0.3 m and the cylinder ratio is 3. The axial inlet is 1 m in length and 0.172 m in diameter. The burner cylinder are connected to the axial inlet by a frustum along 0.5 m. The tangential inlet was placed on the bottom of the frustum. The depths of the tangential inlet (t) were varied in the rank of 0.02, 0.03, 0.04, 0.05, 0.06, 0.07, and 0.08 m, while the tangential inlet width (l) was kept constant at 0.3 m.

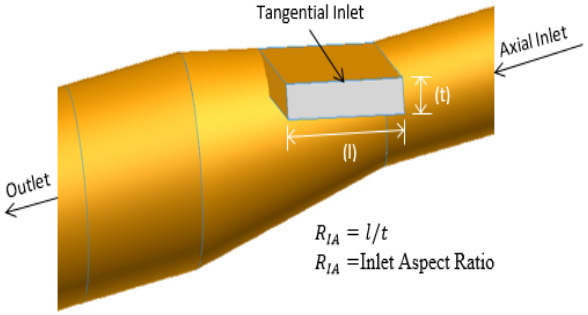

Figure-1. Geometry of tangential burner.

The ratio between the tangential inlet width to the tangential inlet depth is called as an inlet aspect ratio (R_{IA}). According to the above values, the inlet aspect ratios (l/t) in this simulation are 15, 10, 7.5, 6, 5, 4.3, and 3.8.

The simulations are performed at the atmospheric pressure with a constant total mass flow rate and a swirl number which are equal to 0.24 kg/s and 2.6, consecutively. The boundary conditions are no slip wall condition and initial values of the variables p, $\bar{u}_x$, $\bar{u}_y$, $\bar{u}_z$, k, and ε on the wall are zero. Meanwhile, the value of the turbulence variables near the wall are determined by using the standard wall function.

The XY plots and the visualizations using contours, vectors and fluid pathlines are used to analyze the fluid flow characteristics. These techniques are very

useful to identify the velocity and the turbulence intensity profiles and to visualize the three dimensional flow characteristics such as a tornado tail like structure, a spurt pattern and so on.

RESULTS AND DISCUSSIONS

Evaluation of CFD numerical parameters

The evaluation of the effect of the numerical parameters on the performance of the standard k-ε turbulence model is performed on a chamber which has a similar geometry to the tangential burner used in this study. The detailed geometry and operating conditions for the purpose of the evaluation study is taken from Chen study as a high swirl flow case [5].

From several numerical parameters that are evaluated, only the mesh interval size that has a significant effect on the model performance. Within the mesh interval sizes that are varied at the values of 3.4%, 6.8%, 10.3%, 17.1% dan 34.2% of the chamber diameter (D_C), the mesh size that is larger than 0.3% D_C produces significant deviations of the predicted results with the experimental data by Chen [5]. While at the mesh size ≤ 6.8% D_C, the simulation results could follow the experimental data, appropriately. The comparison of the velocity profiles between simulations and corresponding experimental data for several mesh interval sizes are shown in Figure-2.

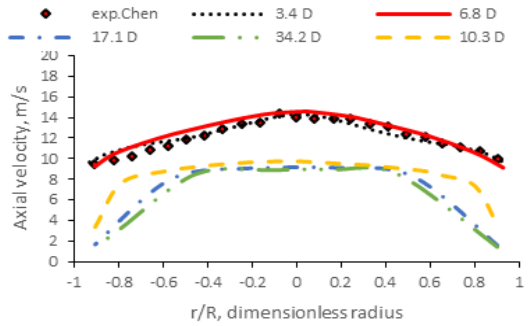

a). Axial velocity profile.

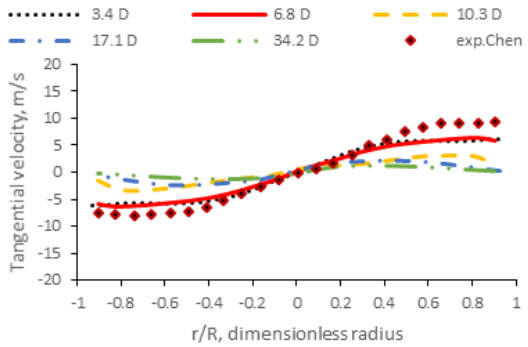

b). Tangential velocity profile.

Figure-2. Present predicted results comparing to Chen experimental data [5] at various mesh sizes.

The numerical parameter study above leads to the set of the numerical parameters to be employed by the next simulation study. The set of the numerical parameters is summarized in Table-1.

Table-1. CFD numerical parameters.

Numerical Parameter	Value			
Mesh Shape	Equilateral Rectangular			
Mesh Size	≤7 % of Burner Diameter			
Pressure-Velocity Coupling Scheme	SIMPLE			
Spasial Discretization Scheme	Pressure	Velocities	k	ε
	Second order	Second order	First order	First order
Wall Function	Standard Wall Function			

Recirculation flow pattern

The internal recirculation flow pattern can increase the degree of the fluid mixing. This pattern is identified from XY plots, and the contour plots, vector plots and three dimensional pathline travels.

Velocity profile

A preliminary identification of the internal recirculation flow is shown by the XY plot of the axial velocity profiles. The existence of this flow pattern is identified by the negative value of the axial velocity. The XY plots of the axial velocity for several R_{IA} values, at two-thirds of the burner cylinder length, are given in Figure-3.

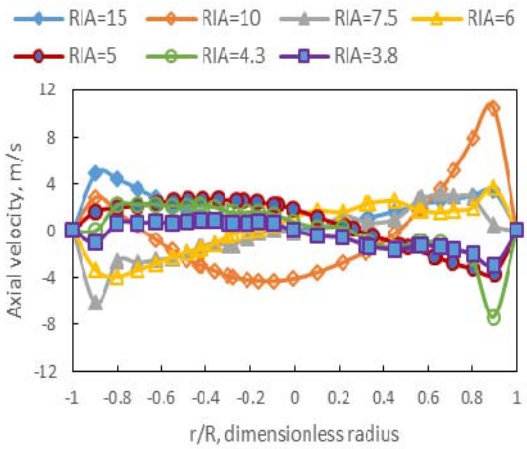

Figure-3. The axial-velocity profiles for several R_{IA} values (at z = 2/3 of burner length).

The figure above reveals that the axial velocity profiles in a tangential burner are significantly influenced by the inlet aspect ratio. At two-thirds of the burner length, the internal recirculation flow exists at all values of R_{IA} except at R_{IA}= 15. The symmetrical recirculation flow

pattern is formed in the burner at the R_{IA} value of 10 that is named as tornado tail like flow structure.

Velocity vectors

To determine the recirculation flow pattern in detail, then the velocity magnitude vectors along the isosurface of the burner are generated. They are shown in Figure-4. The velocity vectors clearly show that internal recirculation flow pattern along the burner are different from each value of R_{IA}. The best penetration of the internal recirculation flow is found at at the R_{IA} value of 10. The internal recirculation flow grows up until the inlet zone of the burner. The deeper the penetration of the internal recirculation flow, the better the flame stability and the chemical conversion are [6].

The recirculation flow from the boiler furnace cause a portion of the flames or the hot flue gas to flow back into the burner. This helps the temperature inside the burner is always maintained as high as it is needed. A high temperature is one of the expected conditions in the burner in order to get the high intensity of the combustion process [3].

Tornado tail like pattern

One of the important internal recirculation flow structure is a tornado tail like flow structure. This is shown in Figure-5.b. This flow pattern is identified through the visualization of the three dimensional flow pathlines. These flow pathlines in the tangential burner, for several R_{IA} values, are shown in Figure-5.

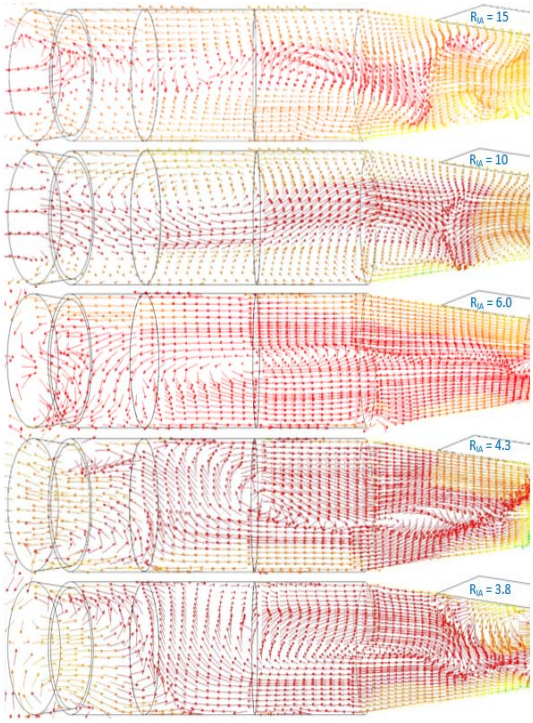

Figure-4. The velocity magnitude vectors along the tangential burner for several R_{IA} values.

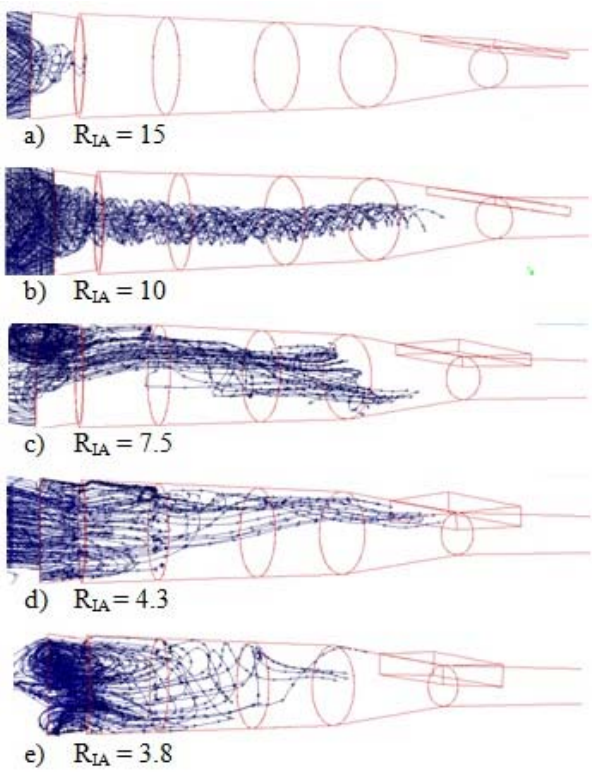

Figure-5. Three dimensional flow pathlines in the tangential burner for some R_{IA} values (at S_n = 2.6 and W_T = 0.24 kg/s).

At the swirl number (Sn) value of 2.6 and the total mass flow rate (W_T) at 0.24 kg/s, it is found that the tornado tail likes pattern is formed at the R_{IA} value of 10. Nemoda results [6] concluded that the tornado tail like pattern was only formed at a high swirl number (Sn $\geqslant$ 2.48). The present results show that the tornado tail like pattern is also formed at a lower swirl number (Sn = 0.8).

At a higher total mass flow rate (W_T = 1.05kg/s), the tornado tail like pattern is found in the burner at R_{IA} = 15 and the swirl number at the value of 1.1. This indicate that the formation of a tornado tail like pattern is determined by the inter action between the inlet aspect ratio, the swirl number and the total mass flow rate.

Turbulence Intensity

The turbulence intensity in this study is represented by the mean turbulence intensity which is calculated by averaging the mean turbulence intensity along the axial burner for several radial points. The simulation results show that the mean turbulence intensity is significantly affected by the inlet aspect ratio, as shown by Figure-6.

In the range of the inlet aspect ratio that is varied, the maximum turbulence intensity value is obtained at the inlet aspect ratio of 10. This agrees with the recirculation flow pattern which its best pattern is also found at the R_{IA} =10. Due to the turbulence intensity is an indicator for the degree of mixing, it can be concluded that the best mixing

characteristics in this study are resulted from the burner at the R_{IA} value of 10.

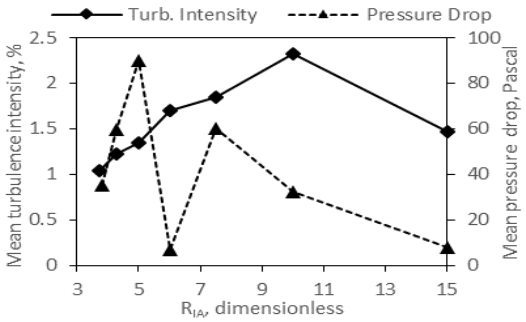

Figure-6. Mean turbulence intensity and pressure drop in a tangential burner for several R_{IA}.

Spurt pattern

The spurt pattern at the burner outlet is influenced by the inlet aspect ratio. The higher the inlet aspect ratio, the more spread out the spurt pattern at the burner outlet is. The spurt patterns at the burner outlet for several inlet aspect ratios are shown in Figure-7.

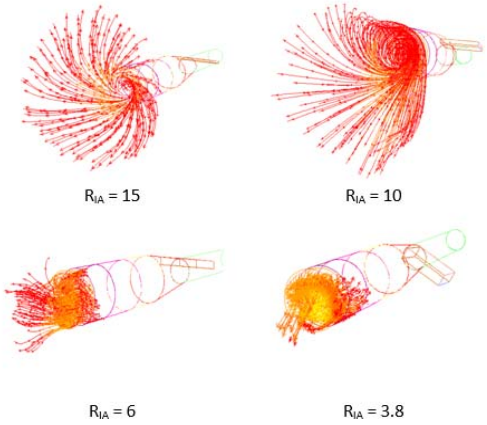

Figure-7. Spurt pattern at burner outlet for several R_{IA} values.

At the R_{IA} values of 10 and 15, the spurt patterns at the burner outlet are spread out well. It looks like a peacock's tail. While at the R_{IA} values 6 and 3.8, the spurt patterns are not spread out well. The spurt pattern, like a peacock's tail, at the burner outlet is better to allow for completing the combustion of the unburnt fuel within the furnace.

Pressure drop

The pressure drop is also quantified in this simulation. This variable is associated with the burner performance namely the operating cost. The higher the pressure drop, the higher the operating cost is.

The mean pressure drop is calculated from the difference between the average static pressure at burner inlet and the outlet. The inlet aspect ratio determines the mean pressure drops along the burner. The minimum pressure drop is obtained at the inlet aspect ratio of 6, as can be seen in Figure-6.

CONCLUSIONS

The numerical investigation results on the axial-tangential burner quantify the existence of the tornado tail like flow structure inside the burner chamber. This flow structure is not only influenced by the inlet aspect ratio but also by the initial tangensial intensiity and by the total mass flow. The the spurt pattern at the burner outlet is formed intensively at the higher inlet aspect ratio. The turbulence intensity and the pressure drop are significantly influenced by the inlet aspect ratio. The inlet aspect ratio of 10 produces better mixing characteristics than others.

ACKNOWLEDGEMENTS

Our thanks go the Ministry of Research, Technology and Higher Education of the Republic of Indonesia for the funding support provided to the implementation of this research.

REFERENCES

[1] S. Tokarski, K. Glod, M. Sciazco, and J. Zuwala. 2015. Comparative assessment of the energy effects of biomass combustion and co-firing in selected technologies. Energy, XXX: 1-9.

[2] L. Siyi, X. Bo, H. Zhiquan, L. Shimming, and H. Maoyun. 2010. Experimental study on combustion of biomass micron fuel (BMF) in cyclone furnace. Journal of Energy Conversion and Management. 51: 2098-2102.

[3] P.K. Nag. 2002. Power Plant Engineering, 2nd ed. McGraw Hill Company, Singapore.

[4] Ansys Inc., Ansys Documentation: Solver Theory. 2013.

[5] J. Chen, B.S. Haynes, and D.F. Fletcher, 1999. "A numerical and experimental study of tangentially injected swirling pipe flow. Proceeding of Second International Conference on CFD in the Minerals and Process Industries CSIRO. Melbourne, Australia. 485-490.

[6] S. Nemoda, V. Bakic, S. Oka, G. Zivkovic, and N. Crnomarkavic. 2005. Experimental and numerical investigation of gaseous fuel combustion in swirl chamber. International Journal of Heat and Mass Transfer. 48: pp 4623–4632.

[7] M.P. Escudier, A.K. Nickson, and R. J. Poole. 2006. Influent of outlet geometry on strongly swirling turbulent flow through a circular tube. Phys of Fluids, 18: 125103.1 - 125103.18.

[8] J. A. R. Vazquez. 2012. A computational fluid dynamics investigation of turbulent swirling burners. Thesis. University of Zaragoza, Spain.

[9] J.F. Bourgouin, J. Moeck, D. Durox, T. Schuller, and S. Candel. 2013. Sensitivity of swirling flows to small changes in the swirler geometry. Comptes Rendus Mecanique. 341: 211–219.

[10] L.C.B.S. Reis, J.A. Carvalho Jr., M.A.R. Nascimento, L.O. Rodrigues, F.L.G. Dias, and P.M. Sobrinho. 2014. Numerical modeling of flow through an industrial burner orifice. Applied Thermal Engineering. 67: 201- 213.